Proceedings of FEDSM'03
2003 4TH ASME_JSME Joint Fluids Engineering Conference
July 6-11, 2003, Honolulu, Hawaii USA

FEDSM2003-45455

SIMILARITY FORMULATIONS FOR TURBULENT BOUNDARY LAYERS AT HIGH REYNOLDS NUMBERS

Gary J. Kunkel
Ivan Marusic
Department of Aerospace Engineering and Mechanics
University of Minnesota
Minneapolis, Minnesota 55455
Email: marusic@aem.umn.edu

ABSTRACT

Data obtained from the high Reynolds number atmospheric boundary layer are used to analyze existing mean-flow and turbulence intensity similarity formulations. From the results of this analysis a new streamwise turbulence intensity formulation is proposed that is suggested to be applicable across the entire smooth-wall high Reynolds number turbulent boundary layer. The new formulation is also shown to be consistent with the mixed-flow scaling suggested by other studies.

NOMENCLATURE

Re_τ Reynolds number based on friction velocity ($\frac{U_\tau \delta}{\nu}$)
R_θ Reynolds number based on momentum thickness ($\frac{U_1 \theta}{\nu}$)
u Fluctuating streamwise velocity
U Mean streamwise velocity
U_1 Freestream velocity
U_τ Wall friction velocity
w Fluctuating wall-normal velocity
z Wall-normal position
δ Boundary layer thickness
θ Momentum thickness
ν Kinematic viscosity

INTRODUCTION

Turbulent boundary layers play an important role in the design and development of many engineering applications involving flowing fluids. For example, they determine the skin friction on vehicles and have an important influence of the dispersion of pollutants in the atmosphere. In most physically realistic applications these boundary layers are at high Reynolds over hydrodynamically rough walls. However, much of the existing experimental data is from low to moderate Reynolds number boundary layers over smooth walls. This makes it difficult to critique existing similarity formulations from the extrapolation of the available moderate Reynolds number data. To remedy this experiments were conducted in the atmospheric surface layer above the salt flats of the Western Utah desert. The data collected are used to analyze existing mean-flow and turbulence intensity similarity formulations.

Apart from the log-law versus power-law controversy [1, 2], the existence of mean-flow similarity in smooth- and rough-wall boundary layers has generally been agreed upon and found to exist across a broad range of studies. The scaling for turbulence intensity similarity, however, is considerably more contentious. For instance, historically, the wall-normal profile of the streamwise turbulence intensity, when scaled with inner-flow variables (U_τ and ν), is thought to be independent of Reynolds number in the entire wall region (viscous sublayer, buffer layer and logarithmic layer). This view is supported by Mochizuki and Nieuwstadt [3] and is also used in many computational turbulence models. Conversely, Marusic, Uddin and Perry [4] proposed a similarity formulation, based on the attached-eddy hypothesis of Townsend [5], that is dependent on Reynolds number. More recent studies by DeGraaff and Eaton [6] and Metzger and

Klewicki [7] have shown that a mixed scaling of both U_1 and U_τ yields similarity in the inner-wall region (viscous sublayer and buffer layer).

The similarity formulation developed in Ref. [4] was compared to experimental data over a large range of moderately high Reynolds numbers; however, due to lack of experimental data, it was not verified at high Reynolds numbers. Here the formulation of Ref. [4] is tested at high Reynolds numbers and is subsequently extended to be applicable across the entire smooth-wall turbulent boundary layer. A brief discussion of the possible rough-wall effects is included along with a comparison of laboratory rough-wall turbulent boundary layer data from Krogstad and Antonia [8]. The extended formulation is also compared with laboratory data presented in Ref. [6] and is found to be consistent with their suggestion of mixed-flow scaling in the inner region of the boundary layer.

EXPERIMENTAL SETUP

All high Reynolds number data used for this study were collected in the surface layer of the atmospheric boundary layer. The experiments were conducted at the SLTEST (Surface Layer Turbulence and Environmental Science Test) facility located on the western Utah salt flats. A detailed description of the site, as well as a discussion of its advantages, are found in Ref. [9]. Several experimental field studies, spanning four years, were conducted to obtain a data set representative of a canonical high Reynolds number turbulent boundary layer. For the data shown here, the surface roughness was estimated at approximately 10 mm, the effects of which can be seen in the offset of the mean-velocity profiles (Fig. 1). All measurements were taken in the evening as the surface layer passed through neutral stability. The stability parameter, z/L, where z is the wall-normal position and L is the Obukhov length, measured from several sonic anemometers, was positive and less than 0.03 for the highest wall-normal measurement position of 2 m [10,11]. Other studies [12] have shown that for $0 > z/L < 0.1$ the turbulence intensities are independent of the stability parameter. Therefore, any slight buoyancy effects that might exist are assumed to be negligible.

Instantaneous streamwise and wall-normal velocity components were obtained using a wall-normal array of hot wires. The array consisted of two single hot wires and six X-wires held on a stand and positioned from 0.06 to 2.0 m above the surface of the salt flats. The X-wires were calibrated in a designated calibration facility against a Pitot-static probe connected to a 10-Torr MKS pressure transducer. They were calibrated at nine angles for each of seven velocities ranging from $\pm 32^o$ and 1-11 m/s respectively. The hot wires were calibrated at the same time as the X-wires at the zero angle position for each of the seven velocities. For the X-wires, a polar look-up table calibration method was then used to determine the two instantaneous velocity components from the two instantaneous voltage signatures. A fourth-order polynomial curve fit was used for the hot wires. The wires were calibrated before and after each experimental run. The calibrations were interpolated, as a function of temperature, to account for the temperature change in the field between calibration and data acquisition ($\approx 6\ ^{o}$C). All wire filaments were 5μm copper-coated tungsten wires with a 1 mm sensing length. The Kolmogorov length scale is estimated to be approximately 0.5 mm so the conventional wires used are able to resolve most of the length scales in the flow down to the dissipation scale. This is why hot wires are used instead of sonic anemometers that typically have a 10-cm measuring path. Ten wires were operated with an AA Labs ten-channel anemometer and four were operated with a TSI IFA-100 four-channel anemometer. All wires were run at an overheat ratio of 1.7. All sensor signals were conditioned with a Tektronix VX4780 signal conditioner and digitized with a Tektronix VX4244 16-bit resolution digitizer. During data collection all wires were simultaneously sampled at a rate of 10 kHz for 30 min.

RESULTS AND DISCUSSION

The two data sets used to analyze the similarity formulations correspond to Reynolds numbers based on the friction velocity ($Re_\tau = U_\tau \delta/\nu$) of approximately 3.1E6 and 3.8E6. The friction velocity was calculated from the Reynolds shear stress at the first X-wire measuring position above the wall ($U_\tau = \sqrt{-\overline{uw}}$). This method of determining the friction velocity agrees well with direct drag-balance measurements also available at the site during the near-neutral stability [13], which was when all the measurements were taken. The boundary thickness for both data sets was estimated as 200 m based on similar days mini-sodar mean-velocity profiles and wind direction measurements throughout the entire atmospheric surface layer. Any possible effects of this boundary layer thickness estimation will be noted in subsequent discussions.

Mean-flow similarity

The mean-flow measurements, plotted with inner-flow scaling ($z^+ = zU_\tau/\nu, U^+ = U/U_\tau$), can be seen in Fig. 1. Here it is easy to see the shift in the classic smooth-wall logarithmic velocity profile due to the roughness. It has been well established that the mean-velocity profile for rough-wall turbulent boundary layers follows a logarithmic overlap law of the wall form,

$$U^+ = \frac{1}{\kappa}\ln[(z+\varepsilon)^+] + A - \Delta U^+, \qquad (1)$$

where A is the classic log law intercept (5.0), κ is the classic log law slope (0.41), ε is the offset in the origin (zero velocity) of the profile due to the roughness and ΔU^+ is the shift in the velocity

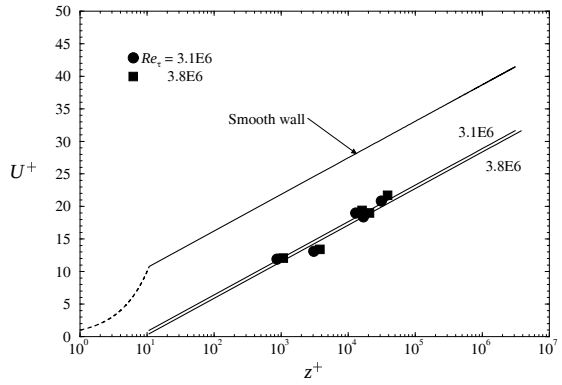

Figure 1. MEAN-VELOCITY MEASUREMENTS. SOLID SYMBOLS ARE DATA FROM THE ATMOSPHERIC SURFACE LAYER. SOLID LINES ARE SMOOTH- ($\kappa = 0.41$ and $A = 5.0$) AND ROUGH-WALL LOG LAWS. DASHED LINE IS THE LAW OF THE WALL.

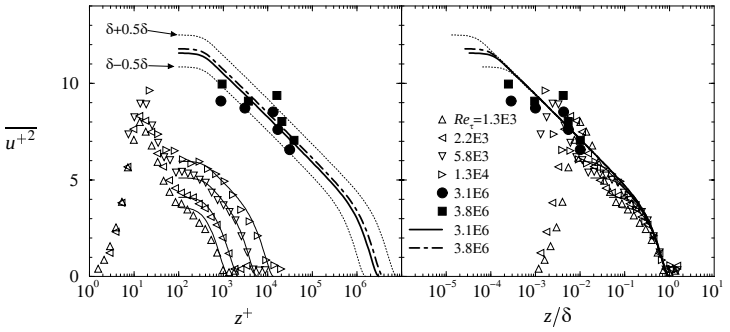

Figure 2. STREAMWISE TURBULENCE INTENSITIES. SOLID SYMBOLS ARE ATMOSPHERIC DATA. OPEN SYMBOLS ARE LABORATORY DATA [6]. SOLID AND DOT-DASHED LINES ARE CORRESPONDING SIMILARITY FORMULATIONS. DOTTED LINES ARE THE SIMILARITY FORMULATION IF THE BOUNDARY LAYER THICKNESS IS 50% LARGER OR SMALLER.

profile due to roughness,

$$\Delta U^+ = \frac{1}{\kappa}\ln[k_s^+] + C. \tag{2}$$

Here k_s is the equivalent sand grain roughness height [14]. Combining Eqns. 1 and 2 yields:

$$U^+ = \frac{1}{\kappa}\ln[\frac{z+\varepsilon}{k_s}] + D, \tag{3}$$

where $D = 8.5$ for $k_s^+ > 70$ [14]. Fitting Eqn. 3 to the mean-velocity profile using a least-squares regression, yields k_s and ε. It is found that $k_s \approx 10$ mm and $\varepsilon \approx 0.8$ mm and -7 mm for the $Re_\tau = 3.1$E6 and 3.8E6 respectively. There is a difference in ε because the stand that the wires were mounted on was repositioned before each run, and therefore, the mean-velocity profile origin with respect to the positions of the wires was changed. The rough-wall logarithmic law of the wall functions corresponding to both Reynolds numbers can be seen in Fig. 1.

Turbulence intensity similarity

The streamwise turbulence intensities from the atmospheric surface layer with inner-flow and outer-flow scaling are shown in Fig. 2 (solid symbols). Similarly, the wall-normal turbulence intensities and the Reynolds shear stresses are shown in Figs. 3 and 4 respectively. In all cases the data from Ref. [6] (open symbols) are also shown for comparison. The Reynolds shear stress behaves as expected for a high Reynolds number flow showing an extended range of approximately constant shear stress.

The corresponding streamwise and wall-normal similarity formulations developed from the attached-eddy hypothesis of Townsend [5] are also shown in Figs. 2 and 3. Extending previous streamwise similarity formulations [15, 16], Ref. [4] developed a formulation, applicable in the entire turbulent wall and outer region of the flow,

$$\overline{u^{+2}} = B_1 - A_1\ln[\frac{z}{\delta}] - V_g[z^+, \frac{z}{\delta}] - W_g[\frac{z}{\delta}]. \tag{4}$$

Here B_1 is a large scale characteristic constant, A_1 is a universal constant, and V_g and W_g are viscous and wake deviations from the logarithmic portion. Details of the development of this formulation can be found in Ref. [4]. Similarly, the wall-normal turbulence intensities are suggested [16] to be described by:

$$\overline{w^{+2}} = A_3 - B_3\frac{z}{\delta} - V_g[z^+, \frac{z}{\delta}], \tag{5}$$

where B_3 is a characteristic constant, A_3 is a universal constant, and V_g is the same as in Eqn. 4. The similarity formulations appear to describe the data well. This suggests therefore, an agreement with Townsend's [5] Reynolds-number-similarity hypothesis. That is, at sufficiently high Reynolds numbers, the turbulence intensities (energy containing motions) are independent of roughness (or viscosity) when scaled with outer-flow variables, insofar as the roughness (or viscosity) may affect the boundary conditions (U_τ).

Recently, however, work has been done with rough-wall turbulent boundary layers [8] that suggests the contrary. Figure 5 shows the streamwise and wall-normal turbulence intensities reproduced from that study with outer-flow scaling for the smooth- and rough-wall boundary layers studied in Ref. [8]. The pluses are the smooth-wall case, and the crosses are the rough-wall case. For comparison the corresponding similarity formulations (dashed lines) and data from Ref. [6] at a similar Reynolds

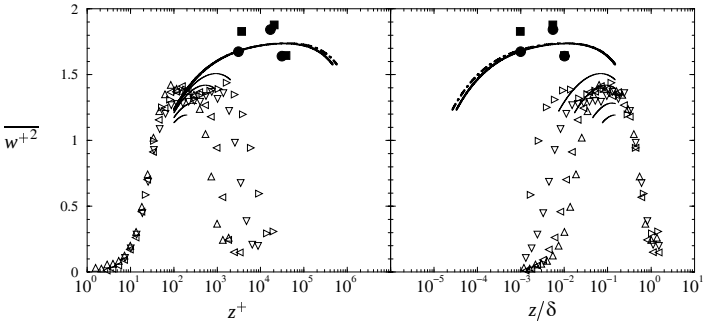

Figure 3. WALL-NORMAL TURBULENCE INTENSITIES. SYMBOLS AS IN FIG. 2.

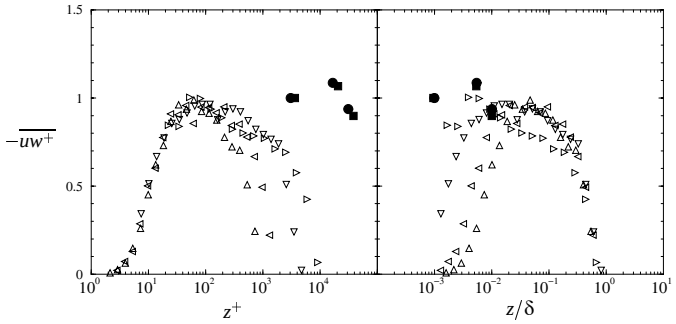

Figure 4. REYNOLDS SHEAR STRESS. SYMBOLS AS IN FIG. 2.

number are also shown here. The Reynolds number and pressure gradients of the smooth- and rough-wall boundary layers are comparable yet while the streamwise turbulence intensities are similar, the wall-normal turbulence intensities for the rough wall show a distinct increase over most of the layer. From the results of that study Ref. [8] conclude that this effect is because of the surface roughness and suggest this is contrary to what one might expect from Townsend's Reynolds-number-similarity hypothesis. However, as previously mentioned, the results from the atmosphere at exceptionally high Reynolds numbers appear to agree with the similarity formulations and Townsend's similarity hypothesis. A possible explanation for this discrepancy is that the Reynolds numbers in the laboratory are not large enough to obtain similarity in the turbulence intensities over the roughness. For instance, while the roughness height scaled with inner variables is similar in both the atmospheric and laboratory studies ($k_s^+ \approx 240$ and $k_s^+ \approx 380$ respectively) the roughness height scaled with the boundary layer thickness is significantly different ($k_s/\delta \approx 0.008\%$ and $k_s/\delta \approx 7\%$ respectively). This seems physically reasonable; at a constant Reynolds number, the larger the roughness elements the further into the layer the effects of the roughness will be felt. Further experimental work is needed to determine the effects of roughness in terms of outer-flow scaling.

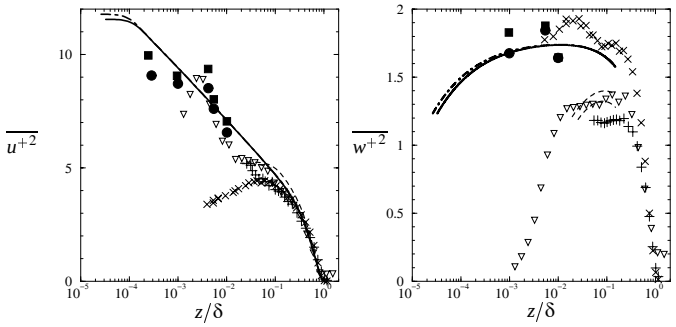

Figure 5. ROUGH-WALL TURBULENCE INTENSITY COMPARISON. SYMBOLS AS IN FIG. 2. PLUSES AND CROSSES ARE LABORATORY (MODERATE REYNOLDS NUMBER) SMOOTH- AND ROUGH-WALL DATA RESPECTIVELY [8]. DASHED LINES ARE CORRESPONDING SIMILARITY FORMULATIONS, EQNS. 4 AND 5.

Extended smooth-wall streamwise similarity formulation

While the existing streamwise similarity formulation (Eqn. 4) appears to describe the data ranging from laboratory to atmospheric Reynolds numbers well, it is only applicable in the log- and outer-region of the flow. Therefore, a new extended similarity formulation in the streamwise direction for flow over a smooth wall is suggested. The following is described in more detail in Ref. [17]. The extended formulation is based on a blending of inner and outer scaling regions that physically represents the outer part of the flow imposing a boundary condition on the inner part of the flow. This forces the inner region to account for the increased level of turbulence, with increasing Reynolds number, in the outer part of the flow. The outer part of the flow ($z^+ > 150$) is described by the existing similarity formulation (Eqn. 4), which is assumed valid for both smooth- and rough-wall boundary layers. The turbulence intensity in the inner part of the flow ($z^+ < 30$) is described by

$$\overline{u^{+2}} = f_1[z^+] f_T[z^+, Re_T], \tag{6}$$

where

$$f_1[z^+] = \frac{0.16(z^+)^2}{\left(1 + a_1(z^+)^2\right)^{1/2} \left(1 + (a_2 z^+)^{2a_3}\right)^{1/2}} \tag{7}$$

is an empirical curve fit of high spatially resolved laboratory data at a moderate Reynolds number, which is valid only for smooth walls. The function f_1 was chosen to have the correct near-wall behavior; $f_1 \to (0.4z^+)^2$ as $z^+ \to 0$. The constants $a_1 = 0.008$, $a_2 = 0.115$, and $a_3 = 1.6$. Here f_T is a scaling function that is linear in $\ln[z^+]$ with a slope proportional to the difference in

Reynolds numbers from the original empirical curve fit. For $z^+ \geq 1$,

$$f_T[z^+, Re_\tau] = 1 + (\alpha - 1)\frac{\ln[z^+]}{\ln[(z^+)_{ref}]}, \tag{8}$$

where α is the value of f_T at $(z^+)_{ref}$, and it is obtained by calculating the ratio of Eqn. 4 (neglecting the viscous and wake deviations) at the desired and reference Reynolds numbers:

$$\alpha = \frac{B_1 - A_1 \ln[(z^+)_{ref}/Re_\tau]}{B_1 - A_1 \ln[(z^+)_{ref}/(Re_\tau)_{ref}]}. \tag{9}$$

Note that, by definition, $z^+/Re_\tau = z/\delta$. For $z^+ < 1$, $f_T = 1$. For simplicity, the inner region and the outer region are blended with a cubic curve fit. Therefore, the entire smooth-wall boundary layer is described by

$$\overline{u^{+2}} = \begin{cases} f_1[z^+]\, f_T[z^+, Re_\tau] & \text{for } z^+ \leq 30 \\ f_2[z^+, Re_\tau] & \text{for } z^+ \geq 150 \\ \text{cubic blend} & \text{for } 30 > z^+ < 150 \end{cases} \tag{10}$$

where f_2 is the original formulation (Eqn. 4). Note, here we tentatively take the limits of the inner and outer regions as $z^+ = 30$ and 150 respectively. The exact values of these limits are of secondary importance.

A graphical representation of this procedure can be seen in Fig. 6. The short dashed lines are the existing Ref. [4] similarity formulations at the reference ($f_2(z^+, (Re_\tau)_{ref})$) and desired ($f_2(z^+, Re_\tau)$) Reynolds numbers. The reference Reynolds number data set (left triangles) was used to calculate the empirical curve fit of Eqn. 7. The empirical curve fit, f_1, is multiplied by the scaling function, f_T, to obtain the formulation for the desired Reynolds number in the lower part of the layer ($z^+ < 30$). This is then blended with the outer formulation at the desired Reynolds number ($f_2(z^+, Re_\tau)$).

The extended formulations, as well as laboratory [6] and atmospheric data, are shown in Fig. 7. Here the formulations for the high Reynolds number atmospheric data are shown as lighter lines because they are not valid in the inner part of the layer due to roughness. However, the extended formulation fits the laboratory data well and suggests that the peak in the turbulence intensity, when scaled with inner-flow variables, increases with increasing Reynolds number. The peak in the turbulence intensity, with inner flow scaling, of the extended formulation as a function of Reynolds number is shown in Fig. 8. The results from the extended similarity formulation agree well with the empirical curve

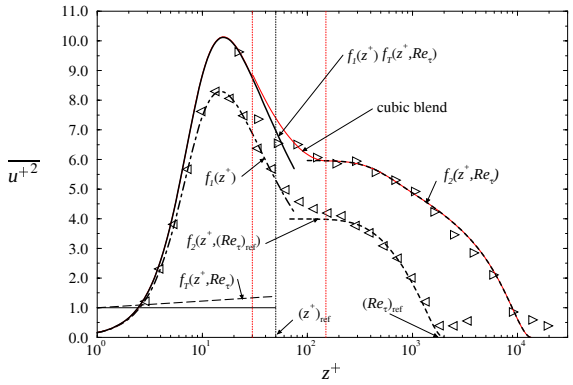

Figure 6. SCHEMATIC OF EXTENDED FORMULATION.

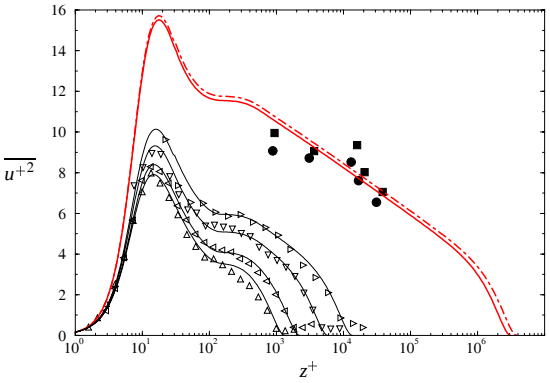

Figure 7. EXTENDED FORMULATION AND EXPERIMENTAL DATA. SYMBOLS AS IN FIG. 2.

fit of high Reynolds number data given by Ref. [7]. Their data was also acquired in the atmosphere, but under smooth-wall conditions.

The extended formulation is also consistent with the mixed scaling suggested in Ref. [6]. Figure 9 shows the formulation, and data, over a range of Reynolds numbers plotted with mixed-flow scaling (U_1 and U_τ). The formulation and data appear to collapse in the inner region of the flow at high Reynolds numbers. This can also be seen by considering the limit of the inner portion of the extended formulation (Eqn. 10) as $Re_\tau \to \infty$.

CONCLUSION

High Reynolds number atmospheric surface layer data have been used to verify mean-flow and turbulence intensity similarity formulations. The streamwise and wall-normal turbulence intensity formulations, based on the attached-eddy hypothesis developed by Refs. [4,16], describe the data well. The effect of the surface roughness ($k_s^+ \approx 240$, $k_s/\delta \approx 8 \times 10^{-5}$) is found not to affect the turbulence intensities in the outer region of the flow, suggest-

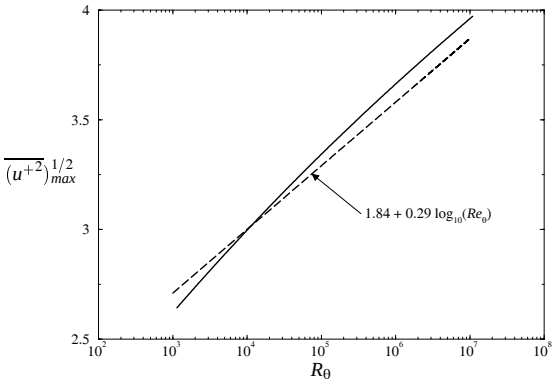

Figure 8. PEAK IN TURBULENCE INTENSITY AS A FUNCTION OF REYNOLDS NUMBER. SOLID LINE CORRESPONDS TO EXTENDED SIMILARITY FORMULATION, DASHED LINE IS FROM REF. [7].

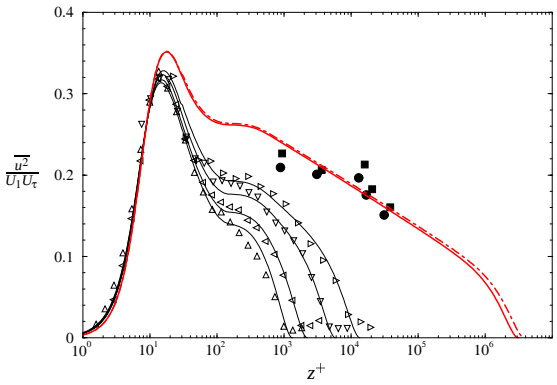

Figure 9. EXTENDED FORMULATION AND EXPERIMENTAL DATA WITH SUGGESTED MIXED SCALING OF REF. [6]. SYMBOLS AS IN FIG. 2.

ing that at sufficiently high Reynolds numbers Townsend's [5] Reynolds-number-similarity hypothesis is valid. The existing formulation of Ref. [4] is extended to be applicable across the entire boundary layer. The extended formulation is found to agree with the empirical mixed-flow scaling proposed in Ref. [6].

ACKNOWLEDGMENT

The authors gratefully acknowledge the financial support of the Packard Foundation and the National Science Foundation under grants CTS-9983933 and ACI-9982274.

REFERENCES

[1] Österlund, J. M., Johansson, A. V., Nagib, H. M., and Hites, M. H., 2000. "A note on the overlap region in turbulent boundary layers". Physics of Fluids, **12** (1), pp. 1–4.

[2] Barenblatt, G. I., Chorin, A. J., and Prostokishin, V. M., 2000. "A note on the intermediate region in turbulent boundary layers". Physics of Fluids, **12** (9), pp. 2159–2161.

[3] Mochizuki, S., and Nieuwstadt, F. T. M., 1996. "Reynolds-number-dependence of the maximum in the streamwise velocity fluctuations in wall turbulence". *Experiments in Fluids,* **21**, pp. 218–226.

[4] Marusic, I., Uddin, A. K. M., and Perry, A. E., 1997. "Similarity law for the streamwise turbulence intensity in zero-pressure-gradient turbulent boundary layers". Physics of Fluids, **9** (12), pp. 3718–3726.

[5] Townsend, A. A., 1976. *The Structure of Turblent Shear Flow*, second ed. Cambridge University Press.

[6] DeGraaff, D. B., and Eaton, J. K., 2000. "Reynolds-number scaling of the flat-plate turbulent boundary layer". *Journal of Fluid Mechanics,* **422**, pp. 319–346.

[7] Metzger, M. M., and Klewicki, J. C., 2001. "A comparative study of near-wall turbulence in high and low Reynolds number boundary layers". Physics of Fluids, **13** (3), pp. 692–701.

[8] Krogstad, P., and Antonia, R. A., 1999. "Surface roughness effects in turbulent boundary layers". *Experiments in Fluids,* **27**, pp. 450–460.

[9] Klewicki, J. C., Foss, J. F., and Wallace, J. M., 1998. "High Reynolds number [$R_\theta = O(10^6)$] boundary layer turbulence in the atmospheric surface layer above Western Utah's salt flats". In Flow at Ultra-High Reynolds and Rayleigh Numbers, R. J. Donnelly and K. R. Sreenivasan, Eds., Springer, pp. 450–466.

[10] Stull, R. B., 1988. *An Introduction to Boundary Layer Meteorology*. Kluwer Academic Publishers.

[11] Kaimal, J. C., and Finnigan, J. J., 1994. *Atmospheric Boundary Layer Flows*. Oxford University Press.

[12] Pahlow, M., Parlange, M. B., and Porté-Agel, F., 2001. "On Monin-Obukhov similarity in the stable atmospheric boundary layer". *Boundary-Layer Meteorology,* **99**, pp. 225–248.

[13] Metzger, M. M., 2002. *Scalar dispersion in high Reynolds number turbulent boundary layers*. PhD thesis, The University of Utah.

[14] Schlichting, H., 1968. *Boundary-Layer Theory*, sixth ed. McGraw-Hill, Inc.

[15] Perry, A. E., and Li, J. D., 1990. "Experimental support for the attached eddy hypothesis in zero-pressure-gradient turbulent boundary layers". *Journal of Fluid Mechanics,* **218**, pp. 405–438.

[16] Hafez, S. H. M., 1991. *The structure of accelerated turbulent boundary layers.* PhD thesis, University of Melbourne, Australia.

[17] Marusic, I., and Kunkel, G. J. "Streamwise turbulence intensity formulation for flat-plate boundary layers". *Physics of Fluids*. Under review.